Carbohydrate Polymers 113 (2014) 438–445

Contents lists available at ScienceDirect

Carbohydrate Polymers

journal homepage: www.elsevier.com/locate/carbpol

Crosslinked bicontinuous biobased PLA/NR blends via dynamic vulcanization using different curing systems

Daosheng Yuan[a], Kunling Chen[a], Chuanhui Xu[a,b,**], Zhonghua Chen[a], Yukun Chen[a,*]

[a] The Key Laboratory of Polymer Processing Engineering, Ministry of Education, China (South China University of Technology), Guangzhou 510640, China
[b] School of Chemistry and Chemical Engineering, Guangxi University, Nanning 530004, China

ARTICLE INFO

Article history:
Received 5 June 2014
Received in revised form 15 July 2014
Accepted 20 July 2014
Available online 30 July 2014

Keywords:
Blends
Curing of polymers
Mechanical properties
Morphology

ABSTRACT

In this study, blends of entirely biosourced polymers, namely polylactide (PLA) and natural rubber (NR), were prepared through dynamic vulcanization using dicumyl peroxide (DCP), sulphur (S) and phenolic resin (2402) as curing agents, respectively. The crosslinked NR phase was found to be a continuous structure in all the prepared blends. The molecular weight changes of PLA were studied by gel permeation chromatography. Interfacial compatibilization between PLA and NR was investigated using Fourier transform infrared spectroscopy and scanning electron microscopy. The thermal properties of blends were evaluated by differential scanning calorimetry and thermogravimetric analysis instrument. It was found that the molecular weight of PLA and interfacial compatibilizaion between PLA and NR showed a significant influence on the mechanical and thermal properties of blends. The PLA/NR blend (60/40 w/w) by DCP-induced dynamic vulcanization owned the finest mechanical properties and thermal stability.

1. Introduction

Currently, biobased polymers issued from renewable resources have received considerable interests from academia and industry, due to their friendly impact on environment. The use of biobased polymers provides a solution to the environment problem of plastic wastes (Armentano et al., 2013; Bordes, Pollet, & Averous, 2009; Auras, Harte, & Selke, 2004). Among various commercial biobased polymers, poly(lactic acid) (PLA) is a promising candidate to some petroleum-based polymers due to its competitive cost, excellent biocompatibility, high strength and modulus (Anderson, Schreck, & Hillmyer, 2008). Moreover, it is derived from renewable resources such as sugar, corn, potatoes, cane, beet and so on (Yu, Dean, & Li, 2006). However, the inherent brittleness of PLA is a major drawback to prevent it from wide application. Many efforts have been done to improve the toughness of PLA. A less expensive and more practical strategy is the melt blending of PLA with other polymers. Various polymers such as, poly(ethylene glycol) (Hu, Hu, Topolkaraev, Hiltner, & Baer, 2003), thermoplastic polyolefin elastomer (Ho, Wang, Lin, & Lee, 2008), polycaprolactone (Sarazin, Li, Orts, & Favis, 2008), polyhydroxyalkanoate copolymers (Schreck & Hillmyer, 2007), polyamide elastomer (Zhang, Chen, & Zhang, 2009), modified soybean oil (Robertson, Chang, Gramlich, & Hillmyer, 2010), ethylene-*n*-butyl acrylate-glycidyl methacrylate terpolymer (EBA-GMA) and a zinc ionomer of ethylene-methyacrylic acid copolymer (EMAA-Zn) (Liu, Song, Chen, Guo, & Zhang, 2011) have been used as toughening modifiers for PLA.

Natural rubber is a renewable resource derived from rubber trees, and known as green elastomer (Rose & Steinbuchel, 2005; Sureerut, Sakdapipanich, & Tanaka, 2009). It possesses excellent toughness, flexibility, biodegradability, biocompatibility, and low cost that makes it a suitable alternative to improve the brittleness of PLA (Bras et al., 2010). Juntuek et al. (2012) used glycidyl methacrylate-grafted natural rubber (NR-g-GMA) as a compatibilizer for PLA/NR blend. Elongation at break and impact strength of PLA/NR blend increased about 2 times and 2.5 times when the NR-g-GMA content increasing to 1% (w/w), respectively. Recently, Bitinis et al. (2012a), Bitinis, Verdejo, Cassagnau, and Lopez-Manchado (2011), Bitinis et al. (2012b) reported the physical blending PLA with NR. Their studies showed that the optimal NR concentration is about 10 wt% which largely improved the brittleness and the elongation at break of PLA. However, to the best of our knowledge, most of the literatures reported on PLA/NR blends are the physical blending of the two components.

We recently reported a super toughened biobased PLA/NR thermoplastic elastomer prepared by dynamic vulcanization using dicumyl peroxide (DCP) as cured agent (Chen, Yuan, & Xu, 2014). It

* Corresponding author at: South China University of Technology, School of Mechanical and Automotive Engineering, The Key Laboratory of Polymer Processing Engineering, Ministry of Education, Wushan RD., Tianhe District, Guangzhou 510640, Guangdong, China. Tel.: +86 02087110804; fax: +86 02085293483.
** Corresponding author at: School of Chemistry and Chemical Engineering, Guangxi University, 100, Daxue Road, Nanning 530004, China.
E-mail addresses: xuhuiyee@gxu.edu.cn (C. Xu), cyk@scut.edu.cn, chenyukun1107@163.com (Y. Chen).

http://dx.doi.org/10.1016/j.carbpol.2014.07.044
0144-8617/

revealed that a continuous structure of the cross-linked NR phase was formed in the blend. The reactive melt blending involved simultaneous cross-linking of NR and interfacial reactive compatibilization between PLA and NR. However, whether the continuous structure of NR phase can be found in PLA by using other curing system? And any changes in mechanical properties of PLA/NR blend with different cure systems? With these aims in mind, this study aims to compare effect of different curing system, namely dicumyl peroxide (DCP), sulphur (S) and paratertiary butylphenol formaldehyde resin (2402), on the structure and properties of PLA/NR blends, and thus obtain the materials with optimized properties for future applications.

2. Experimental

2.1. Materials and sample preparation

Polylactide (PLA), REVODE101 (Zhejiang Hisun Biomaterials Co., Ltd.), MI (190 °C, 2.16 kg) = 5–8 g/10 min, specific gravity = 1.25 g/cm^3; nature rubber (NR), SMRCV60 (Guangzhou Rubber Industry Research Institute, China), Mooney viscosity ML(1 + 4)100 °C = 60 ± 5; dicumyl peroxid (DCP), Sinopharm Chemical Reagent Co., Ltd (China), purified by anhydrous alcohol recrystallization before use. Sulphur (S), Guangzhou Longsun Chemical Co., Ltd (China); Para tertiary butylphenolformaldehyde resin (2402), QingdaoDechen ChemicalCo., Ltd (China); Other chemicals such as Irganox 1010, stearic acid (St), Zinc oxide (ZnO), stannous chloride ($SnCl_2$), 2,2′-dibenzothiazoledisulfde (DM), *N*-cyclohexyl-2-benzothiazolesulfenamide (CZ), were used as received.

The sample codes were defined according to the PLA/NR ratio and cured agent, e.g. the DCP-vulcanized PLA/NR (60/40) blend was defined as DP6R4, the sulphur-vulcanized PLA/NR (60/40) blend was defined as SP6R4, the pata tertiary butylphenol formaldehyde resin-vulcanized PLA/NR (60/40) blend was defined as PP6R4. For all blends, the concentration of Irganox 1010 was fixed at 0.2% weight of (PLA + NR) and the weight ratio of DCP was maintained at 1.5% weight of NR component (i.e., NR/DCP = 100/1.5). For all sulphur-vulcanized blends, the weight ratio of S, ZnO, St, CZ, DM was maintained at 2.5%, 2%, 1%, 0.5%, 1% weight of NR (i.e., NR/S/ZnO/St/CZ/DM = 100/2.5/2/1/0.5/1), respectively. For all paratertiary butylphenol formaldehyde resin-vulcanized blends, the weight ratio of resin, $SnCl_2$ was maintained at 5%, 1% weight of NR (i.e., NR/resin/$SnCl_2$ = 100/5/1), respectively.

PLA pellets were first dried at 80 °C for 6 h in a vacuum oven and NR was masticated. Then the dynamically vulcanized PLA/NR blends were performed by melt blending in a Haake Rheocord 90 at a rotor speed of 60 rpm and at 150 °C. PLA with quantitative Irganox 1010 was firstly shear-melted for 5–6 min and then the masticated NR was added. 5 min later, curing agent was added and the mixing was continued for 5–7 min. Subsequently, the cured blends were removed from the cavity of internal mixer and cooled down to room temperature. After 24 h, the block of the blends was chopped into small granules. The specimens for mechanical properties measurement were prepared by injection molding machine (TTI-160F, Welltec Machinery & Equipment Co. Ltd., China).

2.2. Gel permeation chromatography (GPC)

The solutions of about 3 g blends extraction in chloroform were filtered, followed by the precipitation in excessive cold methanol. The precipitates were dried under vacuum until constant weight at 50 °C temperature for GPC analysis. The weight-average molecular weight (M_w) and molecular weight distribution (polydispersity index (PDI)) of neat PLA and the PLA component from the blends were analyzed using an EC2000 Gel Permeation Chromatography (Dalian Elite Analytical Instruments Co. Ltd., China) with a Shodex GPC column (K-804L) at 25 °C. Chloroform was used at a flow rate of 1.0 mL/min. The samples were dissolved in chloroform with the concentration of 10 mg/mL and injected by 25 μL.

2.3. Fourier transform infrared spectroscopy (FT-IR)

The absorption spectra were recorded using a Bruker Tensor 27 Spectrometer (Germany) with a resolution of 4 cm^{-1} and 32 scans in the waves range 400–4000 cm^{-1}. For the pure PLA and NR, a PLA pellet and a thin film of NR was directly for the FT-IR test using the attenuated total reflectance (ATR) model. For the dynamically vulcanized PLA/NR blends, the free PLA was extracted from blends using Soxhlet extraction apparatus. Samples cut from injection-molded specimens were placed in a thimble holder that was gradually filled with fresh dichloromethane from a distillation flask. A siphon aspirated the solute from the thimble holder upon the liquid reached the overflow level and unloaded it back into the distillation flask. This operation was repeated for 72 h to thoroughly remove the free PLA. Then, a certain amount of the dried insoluble residue, the cross-linked NR, was compressed into thin films for the FT-IR test using the attenuated total reflectance (ATR) model. The trace of PLA in the dried insoluble residue was believed to result from the grafting of PLA onto NR.

2.4. Mechanical properties

Tensile tests were conducted on a universal testing instrument (Shimadzu AG-1, 10KN, Japan) following ISO527-2-1993. The notched impact tests were performed according to ISO 180-2000 using an impact testing machine (ZWICK5331, German, Zwick/Roell) at room temperature. An average value of five replicated specimens was taken for each composition.

2.5. Thermal analysis

Thermal properties were performed using a NETZSCH DSC 204 F1 (German) under an atmosphere of nitrogen. Firstly, about 7–8 mg sampls taken from the center of injection-molded specimens were heated from 30 °C to 180 °C at a rate of 10 °C/min and held at 180 °C for 5 min to eliminate the thermal history. Second, the samples were cooled to −80 °C at a rate of 10 °C/min, holding 3 min at −80 °C, and then heated again to 180 °C at a heating rate of 10 °C/min. The degree of crystallinity (X_c) of PLA component was determined by first heating cycle using the relationship.

$$X_c = \frac{\Delta H_m - \Delta H_{cc}}{\omega_f \Delta H_m^o} \times 100\%$$

where ΔH_m and ΔH_{cc} are the enthalpies of melting and cold crystallization during the heating, respectively; ΔH_m^o is the enthalpy assuming 100% crystalline PLA homopolymers (93.7 J/g) (Garlotta, 2001), and ω_f is the weight fraction of PLA component in the blend.

The thermal stability of the samples (about 5 mg) was investigated with thermogravimetric analysis (TGA) instrument (NETZSCH TG209 F1) under air atmosphere from 30 °C to 800 °C at a heating rate of 20 °C/min. The 5%, 50%, maximum degradation rate weight loss of temperature was denoted as $T_{5\%}$, $T_{50\%}$, T_p, respectively.

2.6. Morphology study

The morphology of the samples was investigated using a Nova NanoSEM 430 field emission scanning electron microscope (FEI,

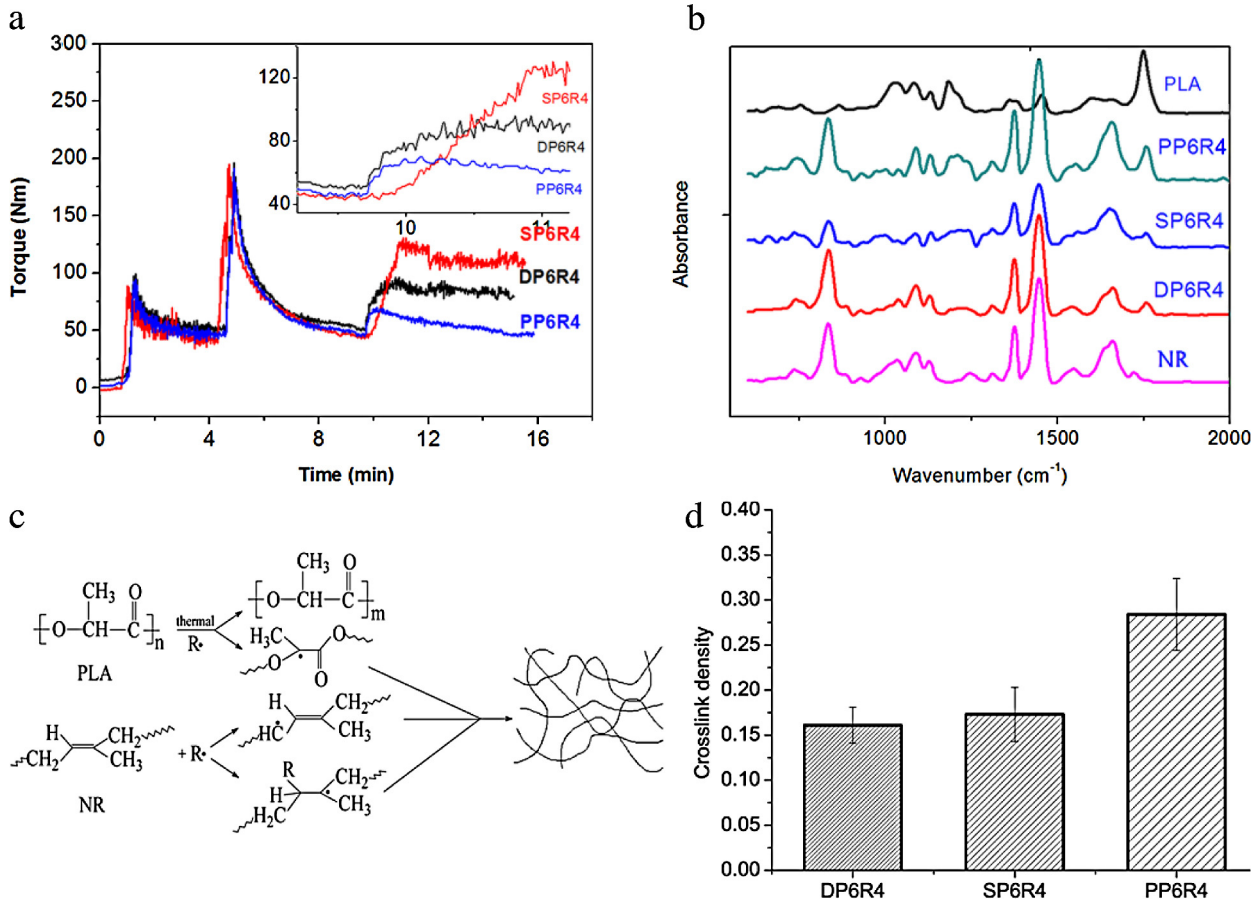

Fig. 1. (a) Melt torque during dynamic vulcanization; (b) FT-IR absorption spectra of individual polymers and residues of DP6R4, SP6R4, PP6R4 extracted by dichloromethane; (c) illustration of the chemical reactions of PLA and NR by initiating free radicals and degradation of PLA; (d) apparent crosslink density of the DP6R4, SP6R4 and PP6R4.

USA). In order to observe the cured NR phase, The cryo-fracture surface of specimens was etched by dichloromethane wash to remove the PLA phase at the surface and then dried sufficiently. The cryo-fracture surface of specimens was obtained from the blend immersed in liquid nitrogen and the impact fracture surface was obtained from the blend after impact strength test. Before morphological observation, the surface of samples was sputter coated with a thin layer of gold.

2.7. Apparent crosslink density of NR phase

The weighed test pieces of blend samples were immersed in toluene at about room temperature for 5d to ensure that swelling equilibrium was reached. Then, the samples were blotted with tissue paper to remove the solvent. The swollen samples were weighed again on an analytical balance. The volume fraction of rubber swollen in the sample gel was used to represent the crosslink density, determined by the following equation:

$$Vr = \frac{1}{1 + \left(m_2/m_1 - 1\right) \times \left(\rho_r/\alpha\rho_s\right)} \quad (1)$$

where m_1 and m_2 are the mass of the sample before and after swollen; ρ_r and ρ_s are the NR and toluene density (ρ_s = 0.865 g/cm^3), respectively; α is the mass fraction of NR in the sample.

3. Results and discussion

3.1. Dynamic vulcanization and reactive interfacial compatibilization analysis

Fig. 1a shows the torque evolution as a function of mixing time for PLA/NR blends with different curing system. The first peak in the torque curve was corresponded to the melting of the PLA pellets and the second peak was due to the melting of NR component. Subsequently, the torque reaches a more or less constant value indicated that the complete melting and full homogenization of the PLA/NR blend. The torque rose after adding curing agent into the melt blend, representing the occurrence of crosslinking. Generally, the slope of torque curve represents the curing rate (Chen & Xu, 2011; Zhang, Zhao, Yuan, Shi, & Zhao, 2010). The difference in the torque curve of PLA/NR blends with different curing system was significant. In case of phenolic resin (2402) system, the slope was the largest and the maximum torque value appeared within 10 s, indicating the curing rate was the fastest. However, the maximum torque value was only about 75Nm and the torque gradually decreased after reaching the maximum value, since the phenonic resin accelerated the degradation of PLA. As for DCP system, the slope was similar to that of phenolic resin in the starting 10 s, but the torque did not change much later. And for the sulphur system, the maximum torque value was as high as to about 125Nm, and the torque curves became relatively flat after attaining the maximum value. This showed that the DCP and sulphur curing system had a limited influence on degradation of PLA.

Table 1
GPC results of PLA component in blends and neat PLAs.

Sample	M_w (g/mol)
Unprocessed PLA	151,900
PLA-150 °C	127,600
DP6R4	122,700
SP6R4	119,900
PP6R4	62,700

Table 1 shows the effects of curing system on the weight-average molecular weight (M_w) of PLA. Compared with the unprocessed PLA, neat PLA processed at 150 °C and PLA in the blends displayed a reduction in molecular weight. Neat PLA processed at 150 °C displayed an approximate 16% reduction in M_w, and PLA in DCP, S curing systems blends displayed an approximate 19% and 21% reduction in M_w, respectively. From above description, it was concluded that the PLA mainly underwent thermal degradation in DCP and sulphur curing system, the curing agents showed small influence on it. However, PLA in the phenolic resin curing system blend underwent approximate 59% reduction in M_w, which is attributed to the alkali in the phenolic resin system that accelerated the degradation of the PLA phase. In fact, the phenolic resins curing agent (Para tertiary butylphenolformaldehyde resin 2402) used in this particular experiment are usually synthesized in the presence of alkaline catalyst. It is well kwon that the alkali can accelerated the degradation of polymer at high temperature. Thus the degradation of PLA chains in phenolic resins system come from two main aspects: (1) thermal degradation induced by high temperature and (2) the trace of residual alkaline catalyst accelerated the degradation of the PLA.

In order to gain insight into the possible reactions between PLA and NR induced by different curing agents, FT-IR spectra were investigated. Fig. 1b shows FT-IR spectra of the individual polymers and residues of the dichloromethane extracted PLA/NR blends recorded in the range of 700–4000 cm^{-1}. The absorption peak at 1750 cm^{-1} is attributed to the stretching vibration of carbonyl groups of PLA. The spectrum of DP6R4, SP6R4, PP6R4 (residues that the PLA/NR blends extracted by dichloromethane for 72 h) was closely identical to that of the pure NR, suggesting that the free PLA component in the PLA/NR blends had been removed completely during dichloromethane extraction. Surprisingly, the absorption peak at about 1757 cm^{-1} was visible for the DP6R4, SP6R4 and PP6R4, confirming that PLA reacted with NR during melt-blending. The extent of the compatibilization reaction between PLA and NR can be approximately described by the amount of grafted PLA per unit of NR, as measured by the ratio of absorption peak area at 1750 cm^{-1} to that at 1735 cm^{-1}, i.e., A_{PLA}/A_{NR}. As shown in Table 2, the A_{PLA}/A_{NR} value of PP6R4 was 0.6862, more than 2-time that of SP6R4, 0.338, and DP6R4 showed a A_{PLA}/A_{NR} value of 0.478. This was showed that the PLA-NR graft ratio in the phenolic resin system was much higher than that in DCP and sulphur curing system. The phenolic resin promoted the degradation of PLA chains and thus resulted in more free radicals which initiated the grafting reaction between PLA and NR. The grafting reaction in sulphur curing system might be attributed to the possible sulphur free radical formed during melt blending at high temperature.

Table 2
FT-IR peak-resolving data of the residues from dichloromethane-extracted dynamically vulcanized PLA/NR blends by different curing system.

Samples	PLA		NR		A_{PLA}/A_{NR}
	ν (cm^{-1})	A_{PLA}	ν (cm^{-1})	A_{NR}	
DP6R4	1758.0	1.461	1375.1	3.059	0.478
SP6R4	1756.3	0.608	1373.4	1.798	0.338
PP6R4	1757.7	2.215	1373.4	3.228	0.6862

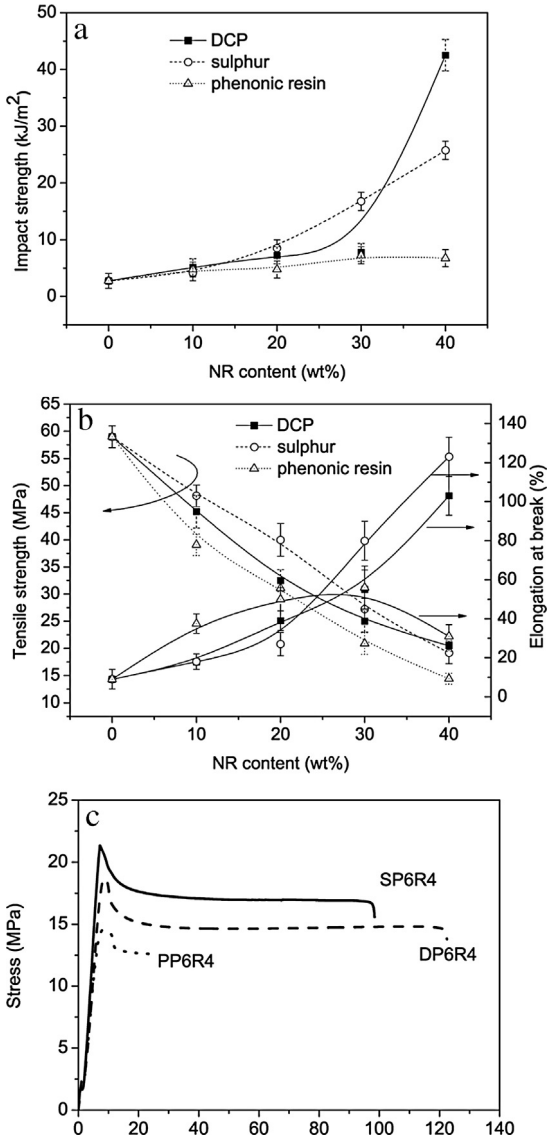

Fig. 2. Mechanical properties of PLA/NR blends as functions of weight content of NR under different curing system.

Table 2 Based on the GPC and FT-IR spectra analysis, the possible crosslinking reaction in PLA/NR blends can be shown in Fig. 1c (Lamb, Anstey, Fellows, Monteiro, & Gilber, 2001; Jin, Lee, Kim, & Yoon, 2000). In phenolic resin system, the PLA was degraded to be smaller molecules, generating lots of free radicals, and thus resulted in the highest PLA-NR graft ratio. The apparent crosslink density of DP6R4, SP6R4 and PP6R4 are shown in Fig. 1d, and the results show that the DP6R4 obtains the lowest crosslink density while the PP6R4 obtains the highest value.

3.2. Mechanical properties

The different curing system shows a significant effect on the mechanical properties of the PLA/NR blends. As shown in Fig. 2a, the impact strength of PLA with 30 wt% NR in phenolic resin system was only 7.25 kJ/m^2, only about 3 times that of the neat PLA. However, the PLA with 40 wt% NR in DCP and sulphur curing systems showed impact strength of 42.5 kJ/m^2 and 25.75 kJ/m^2, about 16 times and 10 times that of the neat PLA, respectively. Similar to most of the toughened PLA blend systems, the tensile strength of

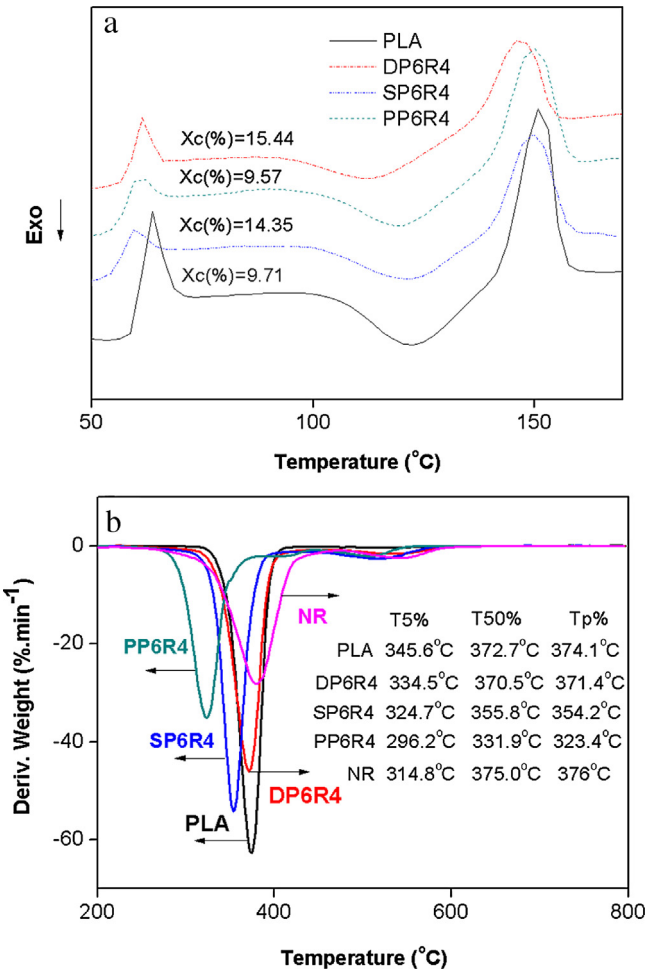

Fig. 3. (a)DSC thermogramic curves of neat PLA and PLA/NR blends during first heating; (b) DTG thermogramic curves of individual polymers and blends under air atmosphere.

the PLA/NR blend cured by various curing agents decreased with the increased NR concentration, and this negative effect was more obvious in phenolic resin system. As shown in Fig. 2b, the elongation at break of the blends was similar to the impact strength, and the blends cured by DCP and sulphur showed a higher elongation than the blends cured by phenolic resin. The stress-strain curves of SP6R4, DP6R4 and PP6R4 are shown in Fig. 2c. The PLA/NR blends cured by DCP and sulphur showed better mechanical properties than that cured by phenolic resin. Especially, the impact strength of the DCP cured PLA with 40 wt% of NR gives marginal increment with the others. According to the FTIR results, the three systems achieved good effective interfacial compatibilization, which facilitated the stress transmission and resulted in high impact strength. However, although the phenolic resin cured blend obtained high graft ratio, the severe degradation of PLA chains in phenolic resin system still lowered the mechanical properties (Fig. 2c). In addition, the network-like NR phase in PLA for the DCP system can effective absorbed the impact energy, further contributed to the high impact strength. This will be shown in Section 3.4.

3.3. Thermal analysis

The mechanical properties of the blends usually were influenced by the crystallinity of the PLA phase. Fig. 3a shows the DSC thermograms of dynamically vulcanized PLA/NR blends with different curing system. The crystallinity of the PLA in blend cured by phenolic resin was closed to that of the neat PLA, while the crystallinities of blends cured by DCP and sulphur were increased to 15.44% and 14.35%, respectively, about 59% and 48% higher than that of neat PLA. The lower crystallinity of the PLA in blend cured by phenolic resin should be attributed to the high graft ratio, which led to a handicap for the alignment of PLA chains during cooling crystallization. It was worth mentioned that the effect of the various curing agent on the impact strength of the blends was consistent with the crystallinity results, which indicated that the crystallinity of the PLA in blend might be one of the factors to influence the toughness of the blends in the present study. The higher crystallinity resulted in a higher impact strength, which was also similar to the report of Oyama (2009).

The thermal stability of neat PLA, neat NR and PLA/NR blends in different curing system was determined by thermogravimetric analysis. The 5% weight loss temperature ($T_{5\%}$), the 50% weight loss temperature ($T_{50\%}$) and fastest decomposition temperature (T_p) of the samples are shown in Fig. 3b. The thermal decomposition of pure PLA begins at 345.6 °C, then reaches its $T_{50\%}$ at 372.7 °C, and its fastest rate at 374.1 °C. Compared with the pure PLA, the $T_{5\%}$, $T_{50\%}$, and T_p of the PP6R4 blend was remarkably decreased to 296.2 °C, 331.9 °C and 323.4 °C, respectively, showing a 49.4 °C, 40.7 °C and 50.7 °C decrease, respectibely. However, the $T_{5\%}$, $T_{50\%}$, and T_p of DP6R4 were 38.3 °C, 38.5 °C and 48 °C higher than that of the PP6D4 blend. From above TGA data, it can be seen that the thermal stability of SP6R4 blend was between that of the DP6R4 and the PP6R4. Based on above descriptions, it can be concluded that phenomic resin curing system greatly reduced the thermal stability of the blend, yet DCP curing system had only a small impact on thermal stability. This difference may be attributed to the sever degradation of PLA induced by phenomic resin.

3.4. Morphology

It is well known that the mechanical properties of multiphase polymer blends depend largely upon the resulting morphologies, thus SEM was using to identify the phase structure of the dynamically vulcanized PLA/NR blends with different curing system. The neat PLA (Fig. 4a) shows a typical brittle fracture surface with no plastic deformation. This is consistence with its poor impact strength of only 2.75 kJ/m^2. No significant interface debonding sign is observed in Figs. 4b and c, showing fine wetting and interactions between the PLA and NR phases. It is clearly seen that the DP6R4 (Fig. 4b) shows a rough surface with obvious plastic deformation, while the PP6R4 (Fig. 4d) shows no plastic deformation. This indicates that the DCP-cured blend achieved better toughness than the phenolic resin-cured blend.

Fig. 5 shows the SEM image of the impact fracture surface of PLA/NR blends with different curing agent. The impact fracture surface of DCP-cured blend illustrates a coarse surface, which is associated to its high impact strength of 42.5 kJ/m^2. The impact fracture surface of sulphur-cured blend left a lot of crevices which contributes to absorb impact energy. As for the phenolic resin-cured blend, it shows an impact fracture surface without apparent plastic deformation, which is similar to its cryo-fracture surface as shown in Fig. 4d, showing low impact strength of only 6.75 kJ/m^2. The above morphologies of the impact fracture surface were consistent well with the impact strength shown in Fig. 2a.

In order to verify that whether the cross-linked NR phase was continuous net-like structure, we used dichloromethane to etch the PLA layer on the cryo-fracture surface of the blends. It is clearly seen from Fig. 6 that the crosslinked NR phase also owned a continuous structure in all the blends cured with different curing system. This structure broke the traditional concept that the sea-island morphology formed after dynamic vulcanization of blends, which had

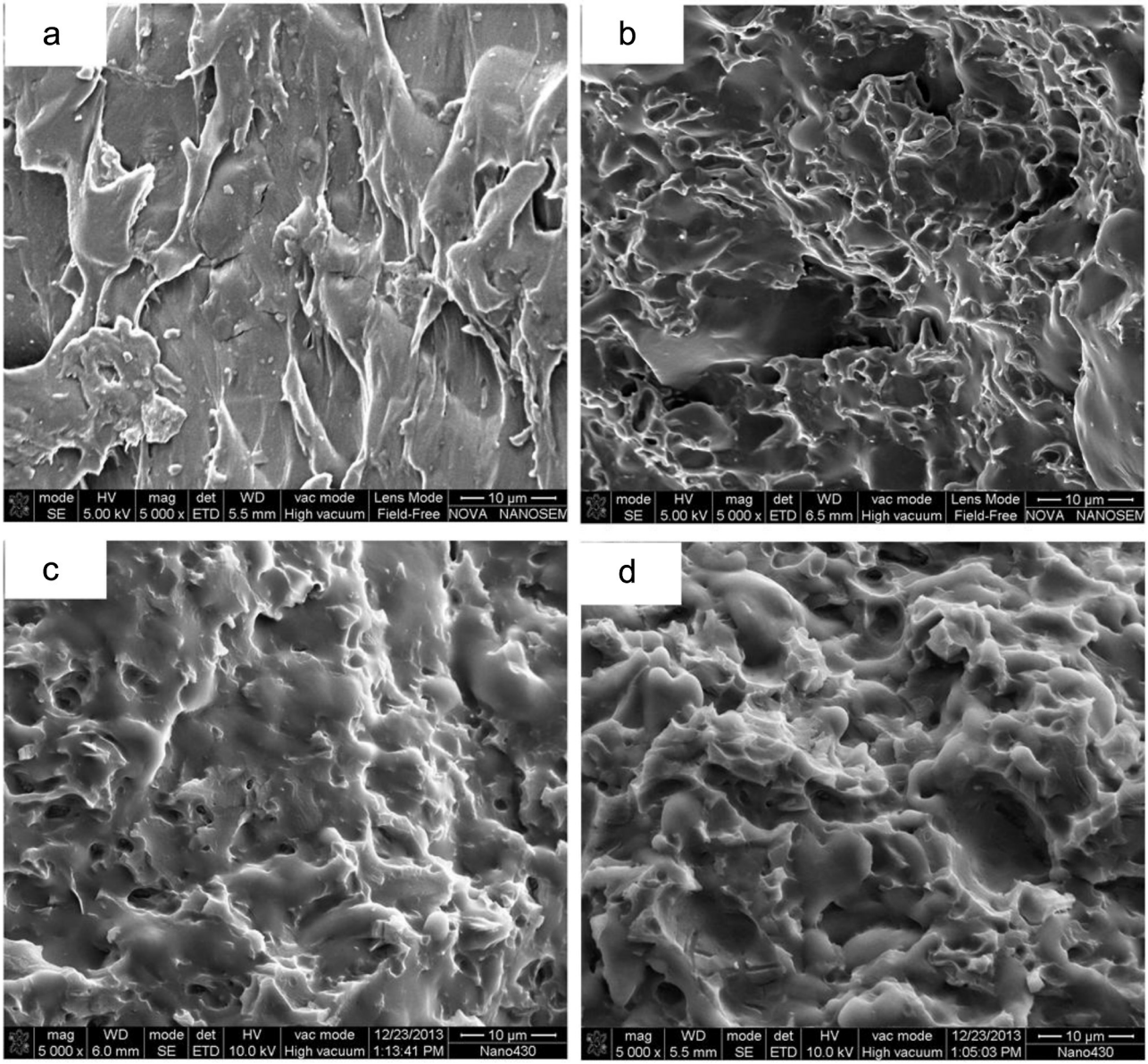

Fig. 4. SEM micrographs of cryo-fracture surface of the pure PLA and dynamically vulcanized PLA/NR blends with different curing system. (a) Pure PLA, (b) DP6R4, (c) SP6R4, (d) PP6R4.

been reported in our previous report (Chen et al., 2014). Generally, the crosslinked rubber phase is in form of dispersed particles in a blend system after dynamic vulcanization. However, the rubber phase is not the dispersed particles but a continuous structure in our blends. In fact, the viscosity of PLA is much lower than the NR at the blending temperature (150 °C) (Chen et al., 2014). The low viscosity of the matrix facilitates the coalescence of the droplets of the NR dispersed phase as the contact time required for drop

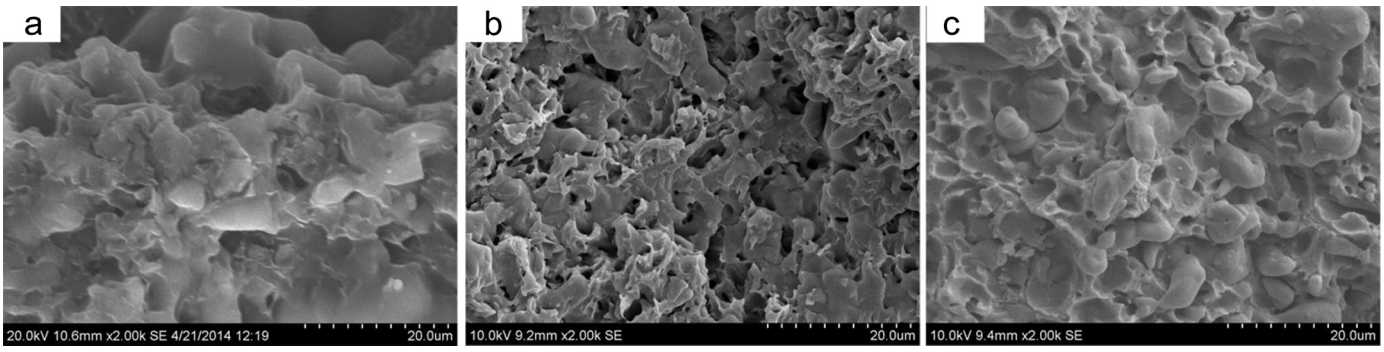

Fig. 5. SEM micrographs of impact fracture surface of dynamically vulcanized PLA/NR blends with different curing system. (a) DP6R4, (b)SP6R4, (c)PP6R4.

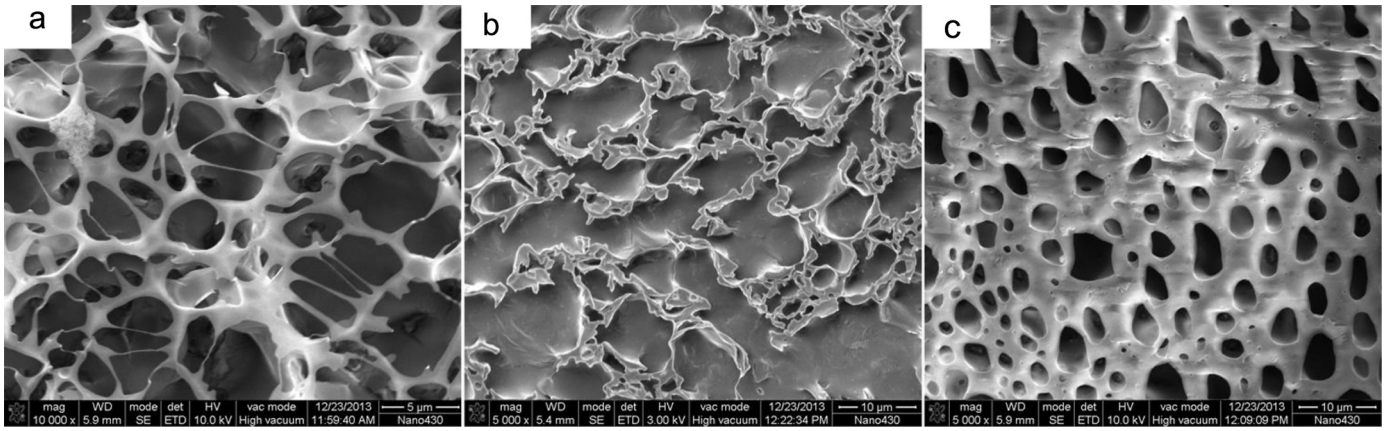

Fig. 6. SEM micrographs of cryo-fracture surface etched by dichloromethane for dynamically vulcanized PLA/NR blends with different curing system.(a) DP6R4, (b) SP6R4, (c) PP6R4.

coalescence is lower. After added the curing agent, the crosslinking increased the strength of NR phase. This might be understood by the fact that if rubber melt strength is much higher than PLA, the PLA continuous phase with much lower viscosity may serve as a lubricated phase to help the rotor slip smoothly between the NR domains, thus forming a crosslinked continuous NR structure. The detailed structure of the NR phase cured with different curing system also showed something differences. The DCP-cured NR seemed to be constructed by thin fibers and formed a network-like morphology structure, like a bone structure throughout the PLA phase. This specific structure, as well as the good interfacial compatibility between PLA and NR phases, should contribute to the high toughness of the blend. The phenolic resin-cured NR looked like bread with lots of holes. This might be due to that the severe degradation of PLA chains weakened the shearing force on the NR phase. According to Wu's theory (Wu, 1987), lowering the matrix viscosity of polymer will result in an increase of size of rubber domains in the blend. In phenolic resin system, the severe degradation of PLA chains further lowered viscosity at the processing temperature, and thus weakened the shearing force on the NR phase, resulting in the observed morphology.

4. Conclusions

This paper studied the effect of DCP, sulphur and phenolic resin curing system on the structure and properties of the PLA/NR blends. The crosslinked NR phase owned a continuous structure in all the blends cured with different curing system. The chemical graft reaction occurred in all the curing systems, which improved the interfacial compatibility between PLA and NR. However, the phenolic resin led to a severe degradation of PLA chains, thus lowered the mechanical properties and thermal stability of the blends. The DCP and sulphur showed a small influence on the degradation of PLA. The PLA with 40 wt% NR in DCP and sulphur curing systems showed notched impact strength of 42.5 kJ/m^2 and 25.75 kJ/m^2, about 16 times and 10times that of the neat PLA, respectively. Compared with the three curing system, the PLA/NR blend (60/40 w/w) by DCP-induced dynamic vulcanization owned the optimum comprehensive properties.

References

Anderson, K. S., Schreck, K. M., & Hillmyer, M. A. (2008). Toughening polylactide. *Polymer Review*, *48*, 85–108.

Armentano, I., Bitinis, N., Fortunati, E., Mattioli, S., Rescignano, N., Verdejo, R., Lopez-Manchado, M. A., & Kenny, J. M. (2013). Multifunctional nanostructured PLA materials for packaging and tissue engineering. *Progress in Polymer Science*, *38*, 1720–1747.

Auras, R., Harte, B., & Selke, S. (2004). An overview of polylactides as packaging materials. *Macromolecular Bioscience*, *4*, 835–864.

Bitinis, N., Sanz, A., Nogale, A., Verdejo, R., Lopez-Manchado, M. A., & Ezquerra, T. A. (2012). Deformation mechanisms in polylactic acid/natural rubber/organoclay bionanocomposites as revealed by synchrotron X-ray scattering. *Soft Matter*, *8*, 8990–8997.

Bitinis, N., Verdejo, R., Cassagnau, P., & Lopez-Manchado, M. A. (2011). Structure and properties of polylactide/natural rubber blends. *Materials Chemistry and Physics*, *129*, 823–831.

Bitinis, N., Verdejo, R., Maya, E. M., Espuche, E., Cassagnau, P., & Lopez-Manchado, M. A. (2012). Physicochemical properties of organoclay filled polylactic acid/natural rubber blend bionanocomposites. *Composites Science and Technology*, *72*, 305–313.

Bordes, P., Pollet, E., & Averous, L. (2009). Nano-biocomposites: Biodegra-dable polyester/nanoclay systems. *Progress in Polymer Science*, *34*, 125–155.

Bras, J., Hassan, M. L., Bruzesse, C., Hassan, E. A., El-Wakil, N. A., & Dufresne, A. (2010). Mechanical, barrier, and biodegradability properties of bagasse cellulose whiskers reinforced natural rubber nanocomposites. *Industrial Crops and Products*, *32*, 627–633.

Chen, Y. K., & Xu, C. H. (2011). Crosslink network evolution of nature rubber/zinc dimethacrylate composite during peroxide vulcanization. *Polymer Composites*, *32*, 1505–1514.

Chen, Y. K., Yuan, D. S., & Xu, C. H. (2014). Dynamically vulcanized biobased polylactide/natural rubber blend material with continuous cross-linked rubber phase. *ACS Applied Materials & Interfaces*, *6*, 3811–3816.

Garlotta, D. (2001). A literature review of poly(lactic acid). *Journal of Polymer and the Environment*, *9*, 63–84.

Ho, C. H., Wang, C. H., Lin, C. L., & Lee, Y. D. (2008). Synthesis and characterization of TPO–PLA copolymer and its behavior as compatibilizer for PLA/TPO blends. *Polymer*, *49*, 3902–3910.

Hu, Y., Hu, Y. S., Topolkaraev, V., Hiltner, A., & Baer, E. (2003). Crystallization and phase separation in blends of high stereoregular poly(lactide) with poly(ethylene glycol). *Polymer*, *44*, 5681–5689.

Jin, H. J., Lee, B. Y., Kim, M. N., & Yoon, J. S. (2000). Properties and biodegradation of poly(ethylene adipate) and poly(butylene succinate) containing styrene glycol units. *European Polymer Journal*, *36*, 165–169.

Juntuek, P., Ruksakulpiwat, C., Chumsamrong, P., & Ruksakulpiwat, Y. (2012). Effect of glycidyl methacrylate natural rubber on physical properties of polylactic acid and natural rubber blends. *Journal of Applied Polymer Science*, *125*, 745–754.

Lamb, D. J., Anstey, J. F., Fellows, C. M., Monteiro, M. J., & Gilber, R. G. (2001). Modification of natural and artificial polymer colloids by topology-controlled emulsion. *Biomacromolecules*, *2*, 518–525.

Liu, H. Z., Song, W. J., Chen, F., Guo, L., & Zhang, J. W. (2011). Interaction of microstructure and interfacial adhesion on impact performance of polylactide (PLA) ternary blends. *Macromolecules*, *44*, 1513–1522.

Oyama, H. T. (2009). Super-tough poly(lactic acid) materials: Reactive blending with ethylene copolymer. *Polymer*, *50*, 747–751.

Robertson, M. L., Chang, K., Gramlich, W. M., & Hillmyer, M. A. (2010). Toughening of polylactide with polymerized soybean oil. *Macromolecules*, *43*, 1807–1814.

Rose, K., & Steinbuchel, A. (2005). Biodegradation of natural rubber and related compounds: Recent insights into a hardly understood catabolic capability of microorganisms. *Applied and Environmental Microbiology*, *71*, 2803–2812.

Sarazin, P., Li, G., Orts, W. J., & Favis, B. D. (2008). Binary and ternary blends of polylactide, polycaprolactone and thermoplastic starch. *Polymer*, *49*, 599–609.

Schreck, K. M., & Hillmyer, M. A. (2007). Block copolymers and melt blends of polylactide with Nodax microbial polyesters: Preparation and mechanical properties. *Journal of Biotechnology*, *132*, 287–295.

Sureerut, A., Sakdapipanich, J., & Tanaka, Y. (2009). Green strength of natural rubber: The origin of the stress-strain behavior of natural rubber. *Journal of Applied Polymer Science*, *111*, 2127–2133.

Wu, S. H. (1987). Formation of dispersed phase in incompatible polymer blends: Interfacial and rheological effects. *Polymer Engineering and Science*, *27*, 335–343.

Yu, L., Dean, K., & Li, L. (2006). Polymer blends and composites from renewable resources. *Progress in Polymer Science*, *31*, 576–602.

Zhang, P., Zhao, F., Yuan, Y., Shi, X. Y., & Zhao, S. G. (2010). Network evolution based on general-purpose diene rubbers/sulfur/TBBS system during vulcanization (I). *Polymer*, *51*, 257–263.

Zhang, W., Chen, L., & Zhang, Y. (2009). Surprising shaped-memory effect of polylactide resulted from toughening by polyamide elastomer. *Polymer*, *50*, 1311–1315.